Structural and electronic properties of Mg, Zn, and Cd from Hartree-Fock and density functional calculations including hybrid functionals

Ulrich Wedig* and Martin Jansen
Max Planck Institute for Solid State Research, Heisenbergstrasse 1, D-70569 Stuttgart, Germany

Beate Paulus
Max Planck Institute for the Physics of Complex Systems, Nöthnitzer Strasse 38, D-01187 Dresden, Germany

Krzysztof Rosciszewski
Institute of Physics, Jagellonian University, Reymonta 4, Pl 30-059 Krakow, Poland

Priya Sony
Atomistic Modelling and Design of Materials, University of Leoben, A-8700 Leoben, Austria
(Received 26 January 2007; published 24 May 2007)

The crystal structures of Zn and Cd deviate from an ideal hexagonal close packing by a significantly increased c/a ratio. In order to investigate the electronic reason for this deviation, especially with regard to the nearly ideal hcp element Mg, Hartree-Fock and density functional theory calculations were performed, employing various functionals within the local density or the generalized gradient approximations as well as hybrid functionals. The cohesive energy, lattice constants optimized with respect to the energy and elastic constants were computed. The role of electronic correlation in consideration of the filled *d*-shell is emphasized, postulating different intra- and inter-layer interactions, both in Zn and Cd. On the potential energy surface in the space of varying lattice constants, a path is explored that corresponds to a uniaxial compression along the *c* axis. In contrast to Mg, the potential energy surface of Zn and Cd is very flat along this path, and an electronic topological transition occurs, leading to a Mg-like band structure.

DOI: 10.1103/PhysRevB.75.205123 PACS number(s): 61.66.Bi, 61.50.Lt, 62.20.Dc, 71.30.+h

I. INTRODUCTION

Among the metallic elements crystallizing in the hexagonal close packed structure, zinc and cadmium stick out conspicuously. The ratios of the lattice constants (Zn: 1.86; Cd: 1.89) deviate considerably from the ideal value (1.63). This fact raises questions about the underlying bonding principles. Triggered by the experiments of Lynch and Drickamer,[1] who measured anomalies in the pressure dependence of the lattice constants as well as of the resistivity of Zn, extensive and partially controversial discussions arose, lasting for the last decade. The anomaly in the pressure dependence of c/a could not be seen in the x-ray diffraction (XRD) results by Schulte *et al.*,[2,3] however, it was confirmed by Takemura, who detected a slope change in the correponding curves at $c/a=\sqrt{3}$ for both Zn (Refs. 4 and 5) and Cd.[5] These publications had a strong impact on the interpretation of subsequent experimental and theoretical results. However, in more recent experiments on Zn, using He as the pressure medium, no anomaly was observed within the limits of experimental error, neither at room temperature[6] nor at low temperatures (40 K).[7–9] The discrepancy with results of the earlier work has been related to nonhydrostatic high pressure conditions. The latest energy-dispersive x-ray diffraction study of Pratesi *et al.*[10] on Cd, using silicon oil as a pressure medium, again shows a slight anomaly in the c/a versus V/V_0 curve. In addition, they observed a shift of the peak position of some Bragg reflections related to the length of the *c* axis. They discussed these shifts in terms of oriented lattice strain and nonhydrostatic effects.

Other properties of Zn showing an anomalous pressure dependence were found in Mössbauer experiments.[11,12] The Lamb-Mössbauer factor (LMF) suddenly drops at 6.6 GPa. The authors attribute this drop to a destruction of a Kohn anomaly due to a change of the topology of the Fermi surface, i.e., an electronic topological transition (ETT). As they point out, this ETT should be accompanied by a softening of low frequency acoustic phonons. Inelastic neutron scattering experiments either support[13] or contradict[14] the interpretation of the Mössbauer data, initiating another debate.[15] In the course of this debate, an alternative cause for the observed drop of the LMF was proposed, a first order transition to a commensurate spin density wave.[16] Raman spectra of the traverse-optical zone-center phonon mode[17,18] showed no anomaly in the pressure range where the LMF drops. However, a change of the sign of slope of the linewidth at $\approx$10 GPa is observed and is attributed to an electronic transition. Computed phonon dispersions[19] are in reasonable agreement with the experiments, but triggered a discussion on the nature of the underlying ETTs.[20,21]

As controversially as the experimental results were discussed, so were the theoretical ones. The main topics of the discussions were the appearance of anomalies in the c/a versus V/V_0 curves and their relations to ETTs, which occur if a conduction band drops below the Fermi level and additional elements appear on the Fermi surface in certain regions of the Brillouin zone. In Zn and Cd, the regions at the *K*- and the *L*-point are of special interest. For Cd an ETT at the *K*-point, leading to "needles" in the Fermi surface, was confirmed by the de Haas-van Alphen experiments.[22] The ETT at

the *L*-point [density functional theory (DFT), local density approximation (LDA)] was considered responsible for the destruction of the Kohn anomaly and thus for the observed drop of the LMF.[12] However, these results are heavily dependent on the choice of the computational parameters.[23–33] Novikov *et al.*[23] have noticed that the equilibrium volume is underestimated by ≈10% when applying the local density approximation (LDA). They proposed several enhancements of the LDA, self-interaction correction, downshift of *d*-states, to improve the results. The best results were obtained at the level of the generalized gradient approximation (GGA) with the PBE functional.[34] Their calculations did not result in an ETT at the *L*-point. In a later work[26] they mentioned another aspect. Slightly beside the minimum of the $E(c/a)$ curve at a given volume, i.e., with a slight deviation from hydrostatic conditions, the lowest conduction band at *L* may fall below the Fermi level. According to Godwal *et al.*,[31] the conduction band at *L* is always lower in the LDA than in the GGA, but always above E_F. This is stated to be true also for finite temperature. Another computational parameter is the number of *k*-points in the Brillouin zone. The influence on the results was also discussed controversially.[28,32] A dense *k*-mesh seems to be necessary especially to find the location of a certain ETT.[33] One should, however, keep in mind that besides the choice of the functional and the number of *k*-points, other computational parameters such as the basis set size, the muffin tin radii, and the linearization energies, also may influence the results and their interpretation.

As pointed out, most of the theoretical work on Zn and Cd was done up to now in order to understand anomalies in the pressure dependence of the lattice constants in terms of electronic topological transitions. Another way to investigate the unusual c/a ratio of Zn and Cd is the application of the bonding principle of optimum hybridization between *s* and *p* valence electrons.[35]

Irrespective of the spread of the results and interpretations reviewed here, all the previous calculations have one common basis: They are performed in the framework of density functional theory. The difficulty in describing the bonding properties of Zn and Cd in a consistent manner may not only be due to inadequate computational parameters, but also due to the limitations of DFT.

To extend the base of knowledge in this regard, in the first part of this work we compared Hartree-Fock (HF) and hybrid functional results with those of DFT calculations, in order to investigate the influence of nonlocal exchange and various approximations of electronic correlation on the results. The comparison with experimental data such as cohesive energies, lattice constants, and elastic constants allowed us to deduce valuable details of the bonding properties of Zn and Cd. We regard this as a first step towards a more rigorous treatment of electronic correlation, which proved to be essential for the description of solid mercury.[36,37] In the second part we investigate the potential energy surface with respect to the lattice constants, PES(a,c), which was probed up to now in areas associated with hydrostatic pressure, now in directions of uniaxial pressure. The unusual behavior of Zn and Cd along this path is discussed in relation to changes of the band structure. In both parts, the results are compared to those of Mg which has formally the same valence electron configuration, but in contrast to Zn and Cd, a nearly ideal c/a ratio.

II. COMPUTATIONAL DETAILS

The calculations were performed with the program package CRYSTAL03.[40] For magnesium we used a crystal optimized all-electron basis set of valence-double-zeta quality including polarization functions. The basis functions of the inner shells were taken from Ref. 41 (*s*) and from Ref. 42 (*p*), which were optimized for the ionic MgO. The diffuse functions especially necessary for the metals also in the *p* channel were optimized for the element. Only in the Hartree-Fock calculations for Mg the exponent of the most diffuse *sp* shell was changed from 0.09 to 0.11 to allow for a larger range of the lattice constants. For Zn and Cd we used scalar-relativistic energy-optimized pseudopotentials with 20 valence electrons, labeled as ecp10mwb (Zn; Ref. 38) and ecp28mwb (Cd; Ref. 39). Thus the semicore *s*- and *p*-orbitals were explicitly treated in the SCF procedure. The corresponding basis sets[38,39] were modified and reoptimized in order to meet the requirements for the use with the CRYSTAL program. The same basis set was applied in connection with a two valence electron pseudopotential [Zn: ecp28sdf (Ref. 43)] which was used to investigate the effect of a frozen *d*-shell in Zn. All the basis sets are summarized in Table I.

The integral tolerances are set to (9 11 9 11 17) for the cutoff parameters ITOL1-5 in CRYSTAL. The shrinking factors defining the *k*-mesh were set to (12 0 24), which corresponds to 133 *k* points in the irreducible Brillouin zone of the hcp lattice. The number of *k* points in the Gilat net is 793. From the energetic point of view, it would be desirable to make the *k* mesh even denser for metals. Increasing the shrinking factors stepwise to (17 0 34) leads to differences in the total energy of about 0.08 eV. However, for calculating the elastic constants it is not possible to use higher shrinking factors, because then, for the calculations of elastic constants which reduce the symmetry, the internal limits of the CRYSTAL03 program are reached. The convergence threshold for the density was set to 10^{-7}, for the pseudopotential to 10^{-9}, for the eigenvalues to 10^{-8}, and for the total energy to 10^{-7}. With these parameters we guarantee that while varying the lattice constants the potential surface is smooth, although in comparison with the experiment the total energy does not have this accuracy.

Some of the calculations on Zn presented here were repeated with the new CRYSTAL06 version,[44] which allows the addition of *f*-basis functions. In these cases the basis set was augmented by a single optimized *f*-function with exponent 0.3.

To compare various representations of exchange and correlation, we performed, besides the pure Hartree-Fock calculations, DFT investigations with various functionals, one LDA (S-VWN: Dirac-Slater exchange,[45] Vosko-Wilk-Nusair correlation[46]) and two GGA functionals (BP86: Becke exchange,[47] Perdew correlation[48] as well as PBE: Perdew-Burke-Ernzerhof exchange and correlation[34]). In addition we applied two hybrid functionals with mixed Hartree-Fock

TABLE I. Crystal optimized Gaussian basis sets for Mg (all electrons), Zn (20 valence electron pseudopotential), and Cd (20 valence electron pseudopotential).

	Mg		Zn		Cd	
	All electrons		20 valence electrons ecp10mwb (Ref. 38)		20 valence electrons ecp28mwb (Ref. 39)	
s	68370.000	0.0002226	30.324127	0.089131	9.727011	−1.7864259
	9661.000	0.0019010	16.316682	−0.124548	7.837523	2.5778948
	2041.000	0.0110420	11.408148	−0.329721		
	529.600	0.0500500	2.569492	0.734637	5.089194	1.0
	159.170	0.1690000				
	54.710	0.3669500	1.40	1.0	1.553326	1.0
	21.236	0.4008000				
	8.791	0.1487000	0.95	1.0	0.714079	1.0
	156.79500	−0.006240	0.15	1.0	0.115	1.0
	31.03390	−0.078820				
	9.64530	−0.079920				
	3.71090	0.290630				
	1.61164	0.571640				
	0.66	1.0				
	0.09	1.0				
p	156.79500	0.007720	111.824980	0.002059	4.742716	−6.2311994
	31.03390	0.064270	19.131910	−0.082381	3.936655	6.5741920
	9.64530	0.210400	5.468838	0.232509		
	3.71090	0.343140	2.505675	0.559404	1.380391	0.7497260
	1.61164	0.373500			0.668485	0.2811080
			1.40	1.0		
	0.65	1.0			0.363423	1.0
			0.95	1.0		
	0.09	1.0			0.125	1.0
			0.15	1.0		
d	0.33	1.0	44.645629	0.047249	8.469341	−0.0163606
			13.438377	0.218926	3.024231	0.2864728
			4.682000	0.452512	1.316367	0.4868518
			1.603211	0.518576		
					0.556393	1.0
			0.482766	1.0		
					0.15	1.0
			0.20	1.0		

(20%) and DFT exchange and DFT correlation (B3LYP: Becke parametrization[49] as implemented in CRYSTAL03 as well as B3PW: same as B3LYP except the use of the nonlocal correlation part of Perdew and Wang[50]). Throughout this work we used the CRYSTAL03 program in order to be able to explicitly calculate the Hartree-Fock exchange and to use hybrid functionals. Therefore we had to use a local Gaussian basis set. To compare to results obtained with an augmented plane wave basis set, calculations with the WIEN2K code[51] were also performed (s,p: LAPW+LO including semicore states; d: APW+lo+LO; $R_{mt}=2.2$; $R_{mt}K_{max}=9.0$; 525 k-points in the irreducible part of the Brillouin zone).

As in the HF case no minimum of PES(a,c) was found, the cohesive energy was always calculated at the experimental lattice constants for comparison. The free atoms are calculated with the CRYSTAL program with two different ap-

TABLE II. Cohesive energies, determined for the experimental lattice constants (eV).

	[a]		Mg	Zn	Cd
Experimental		Ref. 54	−1.50	−1.37	−1.16
HF		This work	−0.36	+0.16	+0.17
		Ref. 55	−0.27		
LDA	S-VWN	This work		−1.65	−1.52
	S-VBH	Ref. 55	−1.80		
GGA	PBE	This work	−1.48	−0.97	−0.77
	BP86	This work		−0.77	−0.62
	BP91	Ref. 55	−1.37		
Hybrid	B3PW	This work	−1.30	−0.82	−0.68
	B3LYP	This work	−0.78	−0.28	−0.20

[a]References to the functionals used are given in Sec. II.

proaches to account for the necessity of more diffuse functions for the free atom: (1) adding one diffuse *sp* shell explicitly in a even tempered manner; or (2) using the crystal basis set and adding 18 ghost atoms in the crystal structure with the same basis set to account for the basis set superposition error. Both approaches differ by only less than 0.03 eV. The difference between the cohesive energy calculated at the experimental lattice constants to the one at the calculated minimum is much larger, e.g., for magnesium in the HF approximation 0.23 eV. The zero point vibrational energies for the metals were also taken into account[52] (Mg: 0.03 eV, Zn: 0.02 eV, Cd: 0.01 eV). The elastic constants presented in the results section were computed according to the procedure described by Fast *et al.*[53] for hexagonal elements. C_{11} and C_{12} were computed via their sum and their difference, which corresponds to a symmetric and an antisymmetric distortion in the *a*-*b* plane, respectively, the latter leading to monoclinic symmetry. C_{33} was obtained by varying the *c* parameter. C_{55} is related to a distortion to a triclinic cell. C_{13} was computed from the relation of the bulk modulus with the elastic constants.

III. RESULTS

A. Cohesive energies

The cohesive energies computed for the experimental lattice constants and the comparison with experimental values are compiled in Table II. For all three elements under examination, common trends have been observed. At the Hartree-Fock level, the calculated cohesive energy of Mg is much too low, Zn and Cd are even not bound at all. The LDA values are generally too high. The best agreement with the experimental value is obtained with the gradient corrected PBE functional. Applying BP86 or the hybrid functional B3PW leads to cohesive energies which are 0.2 eV smaller compared to the PBE results. The deviations are much larger if the hybrid functional B3LYP is used. The cohesive energies are seriously too low. This is astonishing, as both hybrid functionals only differ in the correlation part. This is a first hint that the proper treatment of electronic correlation is crucial for the description of the bonding properties, particularly in Zn and Cd.

TABLE III. Lattice constants. The numbers in each triple correspond to *a* (Å), *c* (Å), and *a*/*c* (italic).

	[a]		Mg	Zn	Cd
Experimental		[b]	3.21 5.21 *1.62*	2.67 4.95 *1.86*	2.98 5.62 *1.89*
HF		This work	3.31 5.09 *1.54*		
		Ref. 55	3.31 5.13 *1.55*		
LDA	S-VWN	This work		2.56 4.88 *1.91*	2.93 5.22 *1.78*
	S-VBH	Ref. 55	3.13 5.00 *1.60*		
GGA	PBE	This work	3.19 5.12 *1.61*	2.65 5.12 *1.93*	3.03 5.52 *1.82*
	PBE	Ref. 57	3.19 5.15 *1.62*		
	BP86	This work		2.63 5.34 *2.03*	3.02 5.58 *1.85*
	BP91	Ref. 55	3.23 5.12 *1.59*		
Hybrid	B3PW	This work	3.19 5.14 *1.61*	2.65 5.10 *1.92*	2.98 5.68 *1.91*
	B3LYP	This work	3.19 5.12 *1.61*	2.65 5.74 *2.17*	3.01 6.04 *2.01*

[a]References to the functionals used are given in Sec. II.
[b]Room temperature values were taken from Ref. 56.

TABLE IV. Bulk moduli and elastic constants; the computed values were determined for the optimized lattice constants, respectively (10^{11} N m^{-2}). The experimental values are taken from Ref. 58.

	[a]	C_{11}	C_{12}	C_{13}	C_{33}	C_{55}	B
Mg	Expt.	0.63	0.26	0.22	0.66	0.18	0.37
	PBE	0.60	0.34	0.21	0.75	0.22	0.39
	PBE[b]	0.65	0.30	0.21	0.75	0.22	0.39
	B3PW[b]	0.70	0.29	0.18	0.76	0.22	0.39
Zn	Expt.	1.79	0.38	0.55	0.69	0.46	0.80
	PBE	1.63	0.53	0.36	0.67	0.26	0.71
	PBE[b]	1.64	0.52	0.36	0.67	0.26	0.71
	B3PW[b]	1.80	0.49	0.43	0.41	0.26	0.75
Cd	Expt.	1.29	0.40	0.41	0.57	0.24	0.62
	PBE	0.70	0.60	0.40	0.58	0.16	0.53
	PBE[b]	0.76	0.55	0.40	0.58	0.16	0.53
	BP86	0.65	0.62	0.41	0.52	0.12	0.52
	BP86[b]	0.73	0.53	0.41	0.52	0.12	0.52
	B3PW[b]	1.36	0.47	0.33	0.45	0.17	0.60

[a]References to the functionals used are given in Sec. II.
[b]Internal relaxation was ignored for symmetry reducing distortions.

B. Lattice constants

The general trends observed for the cohesive energies are reflected by the computed lattice constants (Table III). For Zn and Cd no minimum was found on PES(a,c) at the HF level. In the case of Zn, for c being kept fixed to the experimental value, the optimized a lattice constant is 2.84 Å. The corresponding cohesive energy at this point on the PES(a,c) is +0.03 eV. The enlargement of the a parameter at the HF level points to the importance of electronic correlation on the bonding properties of the elements in the hexagonal layers. Although bound, this is also true for Mg, where the c/a ratio significantly shrinks.

The LDA calculations lead, due to the overbinding, in either case to lattice constants that are too short. The results obtained with gradient corrected or hybrid functionals are not consistent. With all these functionals, the a cell parameter is in very good agreement with the experimental values. The interactions within the hexagonal layers seem to be described rather well by these types of functionals. Concerning c, however, the picture is nonuniform. In the case of Mg, the values are slightly too small, but consistent. For Zn and Cd, the PBE and B3PW results are reasonable, likewise the c parameter of Cd, obtained with BP86. The corresponding value for Zn deviates considerably. Even worse are the values computed with B3LYP. The optimized c parameter has shown to be very sensitive to the treatment of electronic correlation in DFT, which apparently plays a significant role in the bonding properties of the named elements. The unequal dependence of the two respective lattice constants on the correlation functional suggests that the intralayer and the interlayer interactions are of a different nature.

The influence of the filled d-shells on the bonding in Zn and Cd may not be neglected at all. Freezing the d-shell by using the two valence electron pseudopotential leads to drastic changes of the lattice constants (Zn, PBE functional: a =2.95 Å, c=4.63 Å) with a c/a ratio (1.57) even smaller than the ideal one. The discussion of bonding in Zn and Cd on the basis of s-p hybridization, only taking the screening effect of the filled d-shell into account,[35] seems to be insufficient. It is remarkable that the cohesive energy with the two valence electron pseudopotential is much larger (−2.25 eV). So the contributions of the d-shell in the bulk have to be discussed in connection with the corresponding contributions in the isolated atoms.

For Zn, full potential calculations with the WIEN2K code, using the PBE functional, result in lattice constants of a =2.65 Å and c=5.04 Å. The difference in c of 0.08 Å, compared to the CRYSTAL03 result given in Table III, cannot be explained until now. By preliminary calculations with the new CRYSTAL06 code, which allows for the use of f-functions, a significant contribution of polarization functions at the PBE level has been ruled out, as the c parameter thereby changes only by 0.01 Å. The discrepancy between both programs seems to be within the numerical accuracy that can be achieved. For example, the change of the linearization energies of the semicore states in WIEN2K by 1 mRy, which is the accuracy given by the *-in1new* option, will change the total energy by 0.5 meV. This corresponds to a shift on PES(a,c) by about 0.05 Å along the c axis. The double-well structures in the c/a dependence of the energy at certain reduced volumes as discussed by Novikov *et al.*,[23] with barriers of at most 0.4 meV, may also be traced back to numerical effects. The potential energy surfaces computed with CRYSTAL03 are in general less rough. However, we do not claim that the numerical accuracy is significantly better.

C. Elastic constants

The bulk moduli and elastic constants discussed here are given only for those functionals that have led to optimized lattice constants in good agreement with experiment (Table IV). The elastic properties of Mg were analyzed previously by Baraille *et al.*[55] using various functionals. They showed that the reasonable results obtained for the bulk modulus may be due to error cancellation of different erroneous elastic constants, which is especially true at the HF level. The best results they obtained with a gradient corrected functional, which is confirmed by our PBE data. The hybrid functional B3PW yields likewise good results. However, the anisotropy of the elastic properties is less satisfactorily reproduced also by these functionals. Large relative errors occur with elastic constants that are related to a symmetry breaking distortion. For the difference $C_{11}-C_{12}$, which corresponds to an asymmetric distortion in the *a*-*b* plane, the error is −30% at the PBE level, if the relaxation of the atomic positions in the distorted lattice is considered. The error amounts to +22% for C_{55}, where the distorted lattice is triclinic. In this case, the value is less sensitive to internal relaxation. These different responses to internal relaxation in Mg are also found for Zn and Cd.

Whereas for Mg, PBE and B3PW give quite similar results, a different behavior of these functionals is observed with Zn and Cd. With the B3PW hybrid functional, better C_{11} and C_{12} values are obtained, especially for Cd, where the PBE results are rather unsatisfactory. On the other hand, C_{33} computed with B3PW, in contrast to PBE, is considerably too low. This implies that both functionals do not describe the intralayer interaction, being reflected by C_{11} and C_{12}, and the interlayer interaction, which affects C_{33}, in a well-balanced manner. It may be seen as another indication of the different nature of the intra- and inter-layer interactions.

D. Variation of *c* and *a*, band structure

The further investigations on the dependence of the energy in relation to the lattice constants [PES(a,c)] and the analysis of the band structures were done on the basis of calculations with the PBE functional. As pointed out in the Introduction, previously published theoretical work concentrated on the region of PES(a,c) that is related to hydrostatic compression, i.e., points with optimized c/a ratio at a given reduced volume. However, already Novikov *et al.*[26] showed that slightly beside this path, the topology of the Fermi surface may change. In our work we explore another path on PES(a,c) corresponding to uniaxial stress along the *c* axis. In the diagrams in Fig. 1 we plotted the *a* parameter, optimized with respect to the energy, against the *c* parameter as well as the energy PES$[a_{opt}(c),c]$ relative to the global minimum of the potential energy surface. The diagram for Mg [Fig. 1(a)] exhibits the expected shape. The *a* parameter is increasing with shrinking *c*, and the energy dependence is parabolic. The corresponding diagrams for Zn and Cd [Figs. 1(b) and 1(c)] are quite different. In both cases, the increase of *a* is steeper, and the potential energy surface is very flat along this path, featuring even a second local minimum at $a=2.82$ Å and $c=4.40$ Å $(c/a=1.56)$ for Zn. Whether this second minimum is a real physical property of Zn cannot be decided here. As mentioned above, the PBE functional has deficiencies to describe the anisotropy of the elastic properties, and furthermore, the effect is at the limits of accuracy of the program codes used. In the PES computed with the WIEN2K code, no second minimum appears. Nevertheless, the flatness of PES(a,c) along the given path is definitely characteristic for Zn and Cd, at the level of theory applied.

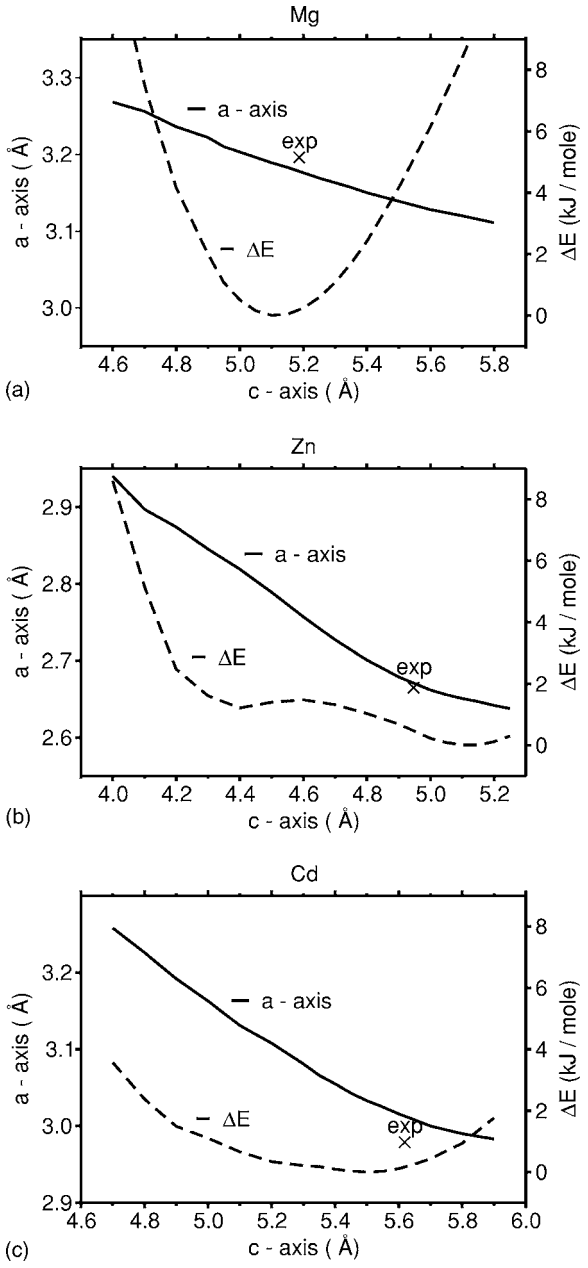

FIG. 1. Optimized *a* parameter as a function of *c* (solid lines) and corresponding energy (broken lines) relative to the global minimum of PES(a,c). The experimental lattice constants are marked by ×(exp).

The band structure of Zn at the global minimum displays remarkable features (Fig. 2, upper left). Besides the fact that the flat *d*-bands cross the valence bands, the latter are degenerate at the Γ-point. The conduction bands stay above the Fermi level at the *L*- and at the *K*-point of the Brillouin zone.

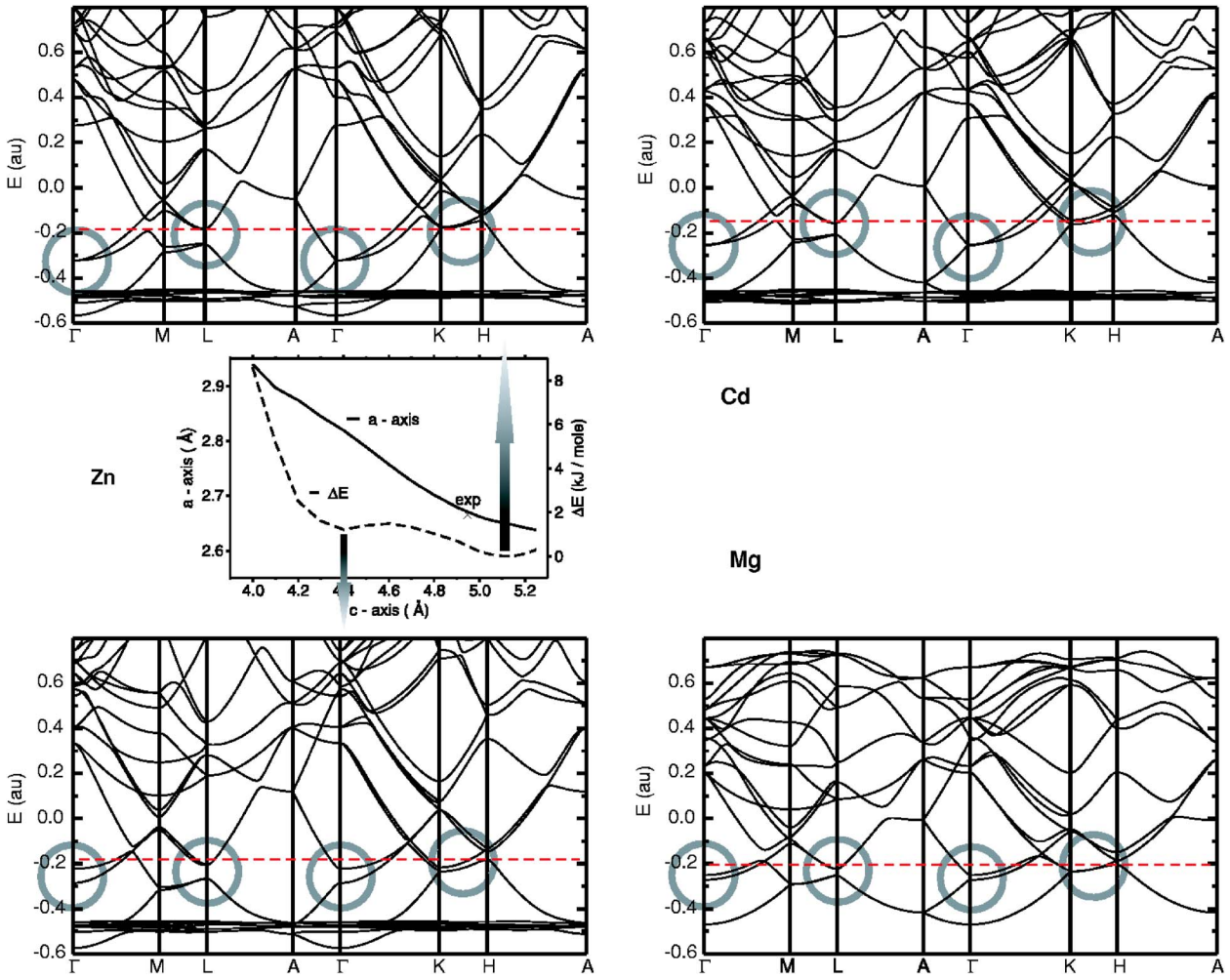

FIG. 2. (Color online) DFT band structure (GGA PBE functional) of Zn (upper left), Cd (upper right), "Mg-like Zn" (lower left), and Mg (lower right). Special regions in the Brillouin zone being discussed in the text are emphasized by circles. The Fermi level is marked by a broken line.

These two features, that are highlighted in Fig. 2 by circles, change along the considered path on PES(a,c). The degeneracy at Γ is lifted and the lowest conduction bands fall below E_F at L and between K and H (Fig. 2, lower left). This means that exactly those ETTs occur, which were discussed controversially in conjunction with the change of the electronic structure under hydrostatic pressure (cf. Introduction). The mentioned dispute may originate from the tiny effect under pressure. Steiner *et al.*[12] quoted an energy difference $\epsilon - E_F$ of only -1 mRy at L ($p \approx 24$ GPa) with a LDA functional, which rather favors the ETT compared to GGA functionals.[31] In our case, at the second local minimum of PES(a,c), the effect is much more pronounced: $\epsilon - E_F$ is -40 mRy at L as well as -62 and -98 mRy at the K-point. With these lattice constants, the band structure and thus the topology of the Fermi surface of Zn is very similar to that of Mg (Fig. 2, lower right), which is why we name it Mg-like Zn. It should be emphasized that the energy difference between real and Mg-like Zn is very low at the PBE level. The band structure at the minimum computed with the two valence electron pseudopotential is, apart from the absent d-bands, virtually identical to the one of Mg-like Zn and thus does not show the properties of the band structure of real Zn. This again indicates that the filled d-shell plays an important role in the bonding in Zn.

The statement that the ETTs may be seen as a driving force for the change of the lattice constants is relativized when examining the band structure of Cd (Fig. 2, upper right). At the global minimum with $c/a = 1.82$, the d-bands just touch the valence bands. In this case, the lowest conduction bands at least partially cross the Fermi level at L and K, although less noticeably (-14 mRy at L and -24 mRy at K) than in Mg-like Zn, and with a certain ambiguity, as the variation of the coefficient κ in the PBE functional, as proposed by Novikov *et al.*,[23] may change this shape of the band structure. One feature of the band structure is common for Zn and Cd at the global minimum and differs from Mg-like Zn and Mg: The highest valence bands around Γ are nearly degenerate.

IV. CONCLUSION

We have compared various properties of Mg, Zn, and Cd obtained from HF or DFT calculations, including hybrid

functionals. At the end, none of the calculations gave entirely satisfactory results. At least the anisotropy of the bonding in Zn and Cd is not described in a well-balanced manner. Apart from the shortcomings, which may be caused by the methods themselves or by their numerical implementation, three conclusions may be drawn from the dependence of the various properties on the method and on the functional used. (1) The anomalous c/a ratio in Zn and Cd is mainly due to electronic correlation. (2) The intra- and inter-layer interactions are different, both in Zn and Cd. (3) The filled d-shell not only screens the nuclear charge in a certain manner, but is explicitely involved in the correlation interactions.

The topology of the Fermi surface of Zn differs significantly from the one of Mg. However, as shown by our calculations, an electronic topological transition can easily be achieved by applying uniaxial pressure along the c axis. From this aspect, the controversy in the discussion of anomalies in the pressure dependence of properties and their relation to ETTs may indeed be traced back to nonhydrostatic conditions in the experiments. Whether the ETTs are really responsible for the unusual c/a-ratio in Zn and Cd is another question. The energy difference between real and Mg-like Zn at the DFT level (GGA, PBE) is rather small and at this level of theory the Fermi surface of Cd shows topological features like that of Mg, even with the large c/a-ratio. In further investigations on Zn and Cd, another aspect must come to the fore, the near degeneracy of the upper valence bands around the Γ-point.

To overcome the current uncertainties related to the methods used, a more accurate treatment of the electronic correlation such as the method of increments[59] is required. Moreover, in order to verify the results obtained from theory, further experiments have to be performed, both to probe the response of the elements to uniaxial stress and to elaborate the relationship between electronic and structural properties.

ACKNOWLEDGMENTS

We acknowledge the support of this work by the priority program 1178 (U.W. and M.J.) of the Deutsche Forschungsgemeinschaft (DFG). Within this program, fruitful discussions with A. Kirfel, H. Schlenz, W. Weyrich, and J. Nuss have to be emphasized.

*Electronic address: u.wedig@fkf.mpg.de

[1] R. W. Lynch and H. G. Drickamer, J. Phys. Chem. Solids **26**, 63 (1965).
[2] O. Schulte, A. Nikolaenko, and W. B. Holzapfel, High Press. Res. **6**, 169 (1991).
[3] O. Schulte and W. B. Holzapfel, Phys. Rev. B **53**, 569 (1996).
[4] K. Takemura, Phys. Rev. Lett. **75**, 1807 (1995).
[5] K. Takemura, Phys. Rev. B **56**, 5170 (1997).
[6] K. Takemura, Phys. Rev. B **60**, 6171 (1999).
[7] K. Takemura, H. Yamawaki, H. Fujihisa, and T. Kikegawa, High Press. Res. **22**, 337 (2002).
[8] K. Takemura, H. Yamawaki, H. Fujihisa, and T. Kikegawa, Phys. Rev. B **65**, 132107 (2002).
[9] K. Takemura, H. Yamawaki, H. Fujihisa, and T. Kikegawa, J. Phys.: Condens. Matter **14**, 10563 (2002).
[10] G. Pratesi, A. Di Cicco, M. Minicucci, and J.-P. Itiè, J. Phys.: Condens. Matter **17**, 2625 (2005).
[11] W. Potzel, M. Steiner, H. Karzel, W. Schiessl, M. Köfferlein, G. M. Kalvius, and P. Blaha, Phys. Rev. Lett. **74**, 1139 (1995).
[12] M. Steiner, W. Potzel, H. Karzel, W. Schiessl, M. Köfferlein, G. M. Kalvius, and P. Blaha, J. Phys.: Condens. Matter **8**, 3581 (1996).
[13] J. G. Morgan, R. B. Von Dreele, P. Wochner, and S. M. Shapiro, Phys. Rev. B **54**, 812 (1996).
[14] S. Klotz, M. Braden, and J. M. Besson, Phys. Rev. Lett. **81**, 1239 (1998).
[15] W. Potzel, Hyperfine Interact. **128**, 151 (2000).
[16] A. W. Overhauser, Phys. Rev. Lett. **81**, 4022 (1998).
[17] H. Olijnyk, A. P. Jephcoat, D. L. Novikov, and N. E. Christensen, Phys. Rev. B **62**, 5508 (2000).
[18] H. Olijnyk and A. P. Jephcoat, Metall. Mater. Trans. A **33A**, 743 (2002).
[19] Z. Li and J. S. Tse, Phys. Rev. Lett. **85**, 5130 (2000).
[20] R. S. Rao, P. Modak, and B. K. Godwal, Phys. Rev. Lett. **87**, 259601 (2001).
[21] Z. Li and J. S. Tse, Phys. Rev. Lett. **87**, 259602 (2001).
[22] S. L. Bud'ko, A. N. Voronovskii, A. G. Gapotchenko, and E. S. Itskevich, Sov. Phys. JETP **59**, 454 (1984).
[23] D. L. Novikov, A. J. Freeman, N. E. Christensen, A. Svane, and C. O. Rodriguez, Phys. Rev. B **56**, 7206 (1997).
[24] L. Fast, R. Ahuja, L. Nordström, J. M. Wills, B. Johansson, and O. Eriksson, Phys. Rev. Lett. **79**, 2301 (1997).
[25] B. K. Godwal, S. Meenakshi, and R. S. Rao, Phys. Rev. B **56**, 14871 (1997).
[26] D. L. Novikov, M. I. Katsnelson, A. V. Trefilov, A. J. Freeman, N. E. Christensen, A. Svane, and C. O. Rodriguez, Phys. Rev. B **59**, 4557 (1999).
[27] N. E. Christensen and D. L. Novikov, Int. J. Quantum Chem. **77**, 880 (2000).
[28] G. Steinle-Neumann, L. Stixrude, and R. E. Cohen, Phys. Rev. B **63**, 054103 (2001).
[29] V. V. Kechin, Phys. Rev. B **63**, 045119 (2001).
[30] P. Modak, R. S. Rao, and B. K. Godwal, J. Phys.: Condens. Matter **14**, 10927 (2002).
[31] B. K. Godwal, P. Modak, and R. S. Rao, Solid State Commun. **125**, 401 (2003).
[32] S. L. Qiu, F. Apostol, and P. M. Marcus, J. Phys.: Condens. Matter **16**, 6405 (2004).
[33] G. V. Sin'ko and N. A. Smirnov, J. Phys.: Condens. Matter **17**, 559 (2005).
[34] J. P. Perdew, K. Burke, and M. Ernzerhof, Phys. Rev. Lett. **77**, 3865 (1996).
[35] U. Häussermann and S. I. Simak, Phys. Rev. B **64**, 245114 (2001).
[36] B. Paulus, K. Rosciszewski, N. Gaston, P. Schwerdtfeger, and H. Stoll, Phys. Rev. B **70**, 165106 (2004).

[37] N. Gaston, B. Paulus, K. Rosciszewski, P. Schwerdtfeger, and H. Stoll, Phys. Rev. B **74**, 094102 (2006).
[38] M. Dolg, U. Wedig, H. Stoll, and H. Preuss, J. Chem. Phys. **86**, 866 (1987).
[39] D. Andrae, U. Haeussermann, M. Dolg, H. Stoll, and H. Preuss, Theor. Chim. Acta **77**, 123 (1990).
[40] V. R. Saunders, R. Dovesi, C. Roetti, R. Orlando, C. M. Zicovich-Wilson, N. M. Harrison, K. Doll, B. Civalleri, I. Bush, Ph. D'Arco, and M. Llunell, *Crystal2003 User's Manual* (University of Torino, Torino, 2003).
[41] N. M. Harrison and V. R. Saunders, J. Phys.: Condens. Matter **4**, 3873 (1992).
[42] M. Catti, A. Pavese, R. Dovesi, C. Roetti, and M. Causà, Phys. Rev. B **44**, 3509 (1991).
[43] G. Igel-Mann, Ph.D. thesis, University of Stuttgart, Stuttgart, 1987.
[44] R. Dovesi, V. R. Saunders, R. Roetti, R. Orlando, C. M. Zicovich-Wilson, F. Pascale, B. Civalleri, K. Doll, N. M. Harrison, I. J. Bush, Ph. D'Arco, and M. Llunell, *Crystal06 User's Manual* (University of Torino, Torino, 2006).
[45] P. A. M. Dirac, Proc. Cambridge Philos. Soc. **26**, 376 (1930).
[46] S. H. Vosko, L. Wilk, and M. Nusair, Can. J. Phys. **58**, 1200 (1980).
[47] A. D. Becke, Phys. Rev. A **38**, 3098 (1988).
[48] J. P. Perdew, Phys. Rev. B **33**, 8822 (1986).
[49] A. D. Becke, J. Chem. Phys. **98**, 5648 (1993).
[50] J. P. Perdew and Y. Wang, Phys. Rev. B **45**, 13244 (1992).
[51] P. Blaha, K. Schwarz, G. K. H. Madsen, D. Kvasnicka, and J. Luitz, *Wien2k, An Augmented Plane Wave+Local Orbitals Program for Calculating Crystal Properties* (Karlheinz Schwarz, Techn Universität Wien, Austria, 2002).
[52] B. Farid and R. W. Godby, Phys. Rev. B **43**, 14248 (1991).
[53] L. Fast, J. M. Wills, B. Johansson, and O. Eriksson, Phys. Rev. B **51**, 17431 (1995).
[54] C. Kittel, *Introduction to Solid State Physics*, 7th ed. (Wiley, New York, 1996).
[55] I. Baraille, C. Pouchan, M. Causà, and F. Marinelli, J. Phys.: Condens. Matter **10**, 10969 (1998).
[56] *CRC Handbook of Chemistry and Physics*, 77th ed., edited by D. Lide (CRC Press, New York, 1996).
[57] L. M. Almeida, C. Fiolhais, and M. Causà, Int. J. Quantum Chem. **91**, 224 (2003).
[58] H. Wern, *Single Crystal Elastic Constants and Calculated Bulk Properties: A Handbook* (Logos Verlag, Berlin, 2004).
[59] B. Paulus, Phys. Rep. **428**, 1 (2006).